www.s2is.org
International Journal on Smart Sensing and Intelligent Systems
ISSN 1178-5608

A LOW COST THREE-DIRECTIONAL FORCE SENSOR

S. Boukhenous

Laboratory of Instrumentation

Faculty of Electronics and Computers

USTHB, Bab_Ezzouar, Algeria, www.lins.usthb.dz

Email: sboukhenous@gmail.com

Submitted: October 20, 2010 Accepted: February 15, 2011 Published: March 1, 2011

Abstract- In this work a low cost sensor has been developed to measure three-directional forces. The theory, design and sensor construction details are presented. It was constructed by using commercial strain gauges. Finite element method was adopted to optimize the structure dimensions, and improve the sensitivity of force sensor by distributing the sensing stress on the maximum strain positions. A hardware conditioning circuits was developed for the 3D force sensor. The calibration experiments were performed to calculate calibration coefficients by using the regression analysis method and test linear property of the sensor.

Index terms*:* Strain gauge, three-directional forces, 3D force platform, gait and posture.

I. INTRODUCTION

The measurement of foot-ground reaction forces produced by human body in biomechanical analysis is very important. Ground reaction measurement with force plates has been devoted to perform dynamics analysis in many environments [1], [2]. A variety of sensor systems have been developed, including resistive strain gauges, piezoelectric film [3], capacitive sensors, Hall effect [4], [5], but in these systems the effects of shearing forces were neglected. Some sensors recently are developed to measure compressive and shear forces at the skin-object interface [6], but the force levels are limited in the measurements of small forces about 50N. Pressure platforms reliably deliver pressure distribution under the foot, foot location, vertical reaction, and displacement of the center of pressure, but they do not give any information about shear forces [7]. Gait and posture analysts sometimes neglect the local components of shear forces because of the great amount of information already delivered by the vertical reaction components [8], [9]. Two multi-dimensional sensors for human dynamics analysis have been introduced in [10], but these structural sensors with load-coupling were difficult to be calibrated. In this paper, we are developing a strain gauge sensor used an easy innovative made instrument for measuring 3D forces during human walking. A finite element method was adopted to optimize the structure dimensions, and improve the sensitivity of force sensor by distributing the sensing stress on the maximum strain positions. After optimization and realization model, hardware conditioning circuits was developed for the 3D force sensor. The calibration experiments were performed to calculate calibration coefficients by using the regression analysis method and test linear property of the sensor.

II. DESIGN OF THE 3D TEST BODY

The 3D test body configuration is depicted schematically in figure.1. The transducer has a proving ring for measuring vertical force F_z and squared portion for measuring the horizontal forces F_x and F_y. These parts were machined separately and assembled together for reducing the complexity of machining the whole sensor.

Figure1. The 3D test body

a. Design of the proving ring

The function of the proving ring is to detect the vertical force component. This provides increased sensitivity and is less to crosstalk from horizontal forces [11]. The proving ring dimensions were selected to provide a safety factor of at least three before fracture failure due to excessive vertical loads. Calculations were carried out to verify the safety of the design and to assure adequate sensitivity. The proving ring was analyzed as a thick-walled circular ring and the vertical force was considered as a vertical load (figure.2). The greatest circumferential stresses which occur at the Section A-A of the ring were found by the formula [12]:

$$\sigma = K.\frac{2p}{\pi \cdot b} \quad (1)$$

Where: p = load/unit length of the ring, and K is a numerical coefficient which depends on the ratio of inside to outside radius, a/b. A positive K indicates tensile stress and a negative K compressive stress. In this proving ring (figure. 2), we have: a = 20 mm, b = 25 mm, c = 20 mm, there for, a/b =0,8.

If the maximum vertical loads F_Z is 800 N, then:

$$p = \frac{F_z}{c} = 40 \text{ N/mm}^2 \quad (2)$$

at points 1 and 3 on the ring, K = +32

at points 2 and 4 on the ring K = -40

The K values were extrapolated from the K versus a/b, table [12]. The stresses at the section A-A points 1, 2, 3, and 4 were estimated as:

$$\sigma_1 = \sigma_3 = 32 \cdot \frac{2.40}{\pi.25} = 32{,}61 \text{ N/mm}^2 \quad (3)$$

$$\sigma_2 = \sigma_4 = -40 \cdot \frac{2.40}{\pi.25} = -40{,}76 \text{ N/mm}^2 \quad (4)$$

Requiring the safety factor of at least three, the safe stress is:

$$\sigma_s = 3.\sigma_2 = 122{,}28 \text{ N/mm}^2 \quad (5)$$

For the aluminum AU4G, the yield tensile strength σ_y is 441 N/mm^2. Since $\sigma_s << \sigma_y$, this ring structure design is safe. The average total stress at the section A-A is:

$$\sigma_a = \frac{\sigma_1 + \sigma_2}{2} = 36{,}68 \text{ N/mm}^2 \quad (6)$$

The average strain is:

$$\varepsilon_a = \frac{\sigma_a}{E} = 5.10^{-4} \quad (7)$$

where E: the Young's Modulus for aluminum AU4G

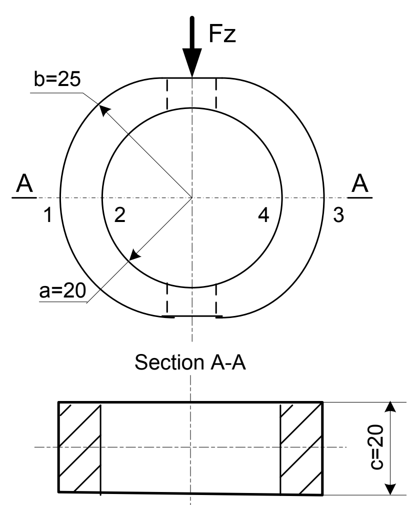

Figure 2. The cross section of the proving ring

b. Design of the squared portion

A squared portion (figure.3) provided a flat surface for mounting gauges to measure horizontal forces *Fx* and *Fy*. The design was used to increase the gauge mounting accuracy, reliability of mounting, and to reduce crosstalk between the horizontal forces. The Total of quadratic moment of the transducer is:

$$I_T = I_s - (2I_2 + 2I_3) \tag{8}$$

where

I_2 : the quadratic moment of the segment about the axis 2-2, I_3 : the quadratic moment of the segment about the axis 3-3, and I_s : the quadratic moment of the hollow shaft,

$$I_s = \frac{\pi.(R^4 - r^4)}{4} = 9739{,}72 \text{ mm}^4 \tag{9}$$

where R =10mm and r = 7mm

$$\begin{aligned} I_2 &= 0{,}133.R^4.\theta^5(1 - 0{,}476.\theta^2 + 0{,}111.\theta^4) \\ &= 22{,}53\text{mm}^4 \end{aligned} \tag{10}$$

$$I_3 = I_1 + S.d^2 \cong S.d^2 = 518{,}67\text{mm}^4 \tag{11}$$

where I_1 : is the quadratic moment of the segment about the axis 1-1, $I_1 << S.d^2$

d: is the distance from the central axis to the principle axis

$$d = d_1 + d_2 = 9 + 0{,}98 = 9{,}98\text{mm} \tag{12}$$

d_2: is the distance from central axis of the segment to the extreme fibre

$$d_2 = 0{,}2.R.\theta^2(1 - 0{,}0619.\theta^2 + 0{,}0027.\theta^4) \tag{13}$$

θ = 25,84° = 0,451rd *and S* : is the segment area

$$S = \frac{2}{3}.R^2.\theta^3.(1 - 0{,}2.\theta^2 + 0{,}019.\theta^4) = 5{,}87\text{mm}^2 \tag{14}$$

The total of quadratic moment of the transducer cross section (figure.3) is:

$$I_T = I_s - (2I_2 + 2I_3) = 8657{,}22\text{ mm}^4 \tag{15}$$

If the maximum horizontal force (F_x or F_y) is 450 N, then the maximum stress on the cross section is

$$\sigma = \frac{F_x.L.d_1}{I_T} = \frac{F_y.L.d_1}{I_T} = 42{,}10\,\mathrm{N/mm}^2 \quad (16)$$

where L = 90 mm is the distance from the center of the strain gauge to the pin joint where the applied vectorial force.

d_1: is one half of the distance between the two flat surfaces of the section (d_1 = D/2=9mm).

If the safety factor is at least 3, then the safe stress should be:

$$\sigma_S = 3\,.\,\sigma = 126{,}3\,\mathrm{N/mm}^2 \quad (17)$$

however the since yield stress σ_y = 441 N/mm^2, then $\sigma_s < \sigma_y$.

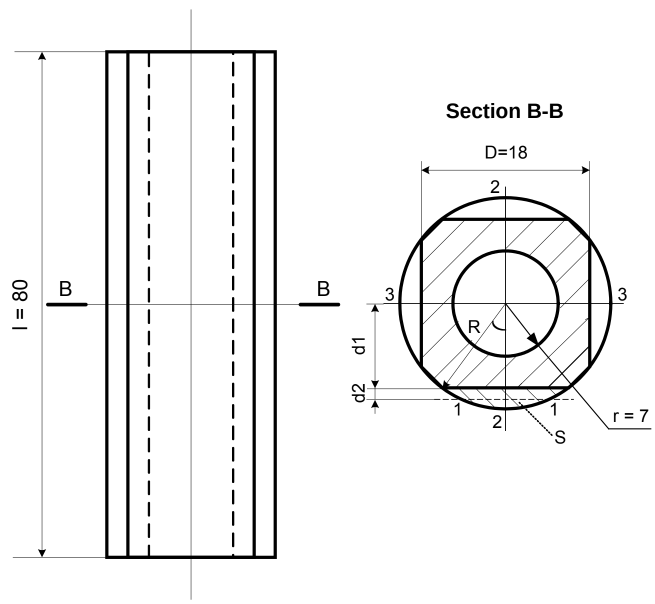

Figure 3. The squared portion and cross section

III. SIMULATION RESULTS OF THE TEST BODY

The simulation of the test body is realized by using a software program ‘SolidWorks’. The stress distribution result of the test body under the effects of shearing forces *Fx* and *Fy* is depicted schematically in figure.4 and figure.5. The shearing forces cause significant deformations on the central and lower part of the squared portion, from where the choice of the emplacement of the strain gauges for measurement the shear forces. In this case the proving ring is not affected.

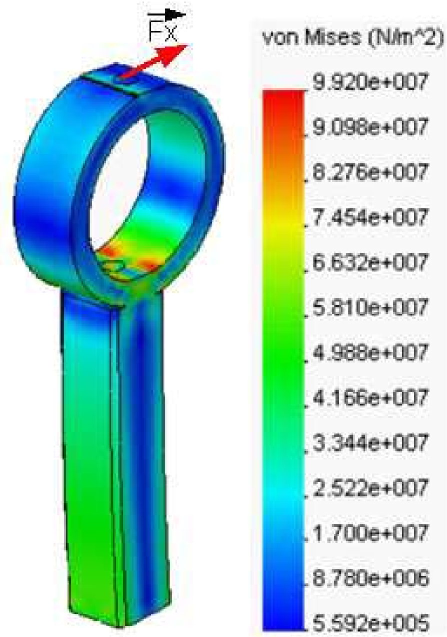

Figure 4. Stress result of *Fx* shearing force

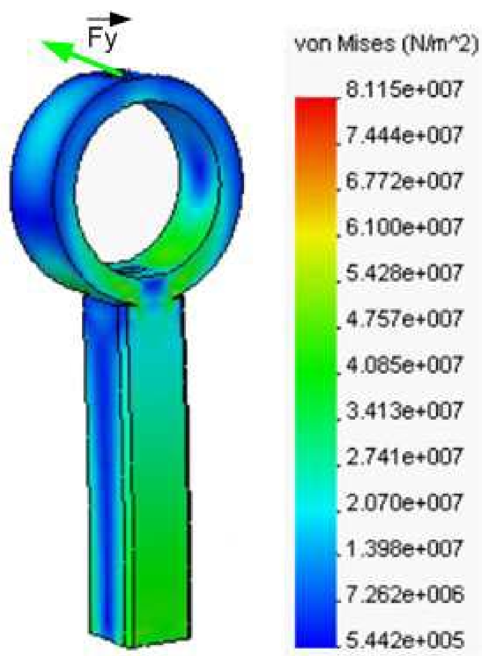

Figure 5. Stress result of *Fy* shearing force

The stress result of the test body under the effect of comprising force *Fz* is depicted schematically in figure.6. According to these results, the stress is sudden by the proving ring only. In more the stress is significant (green zone) on the neutral axis of the ring. From where, the choice emplacement of strain gauges for the compression force detection.

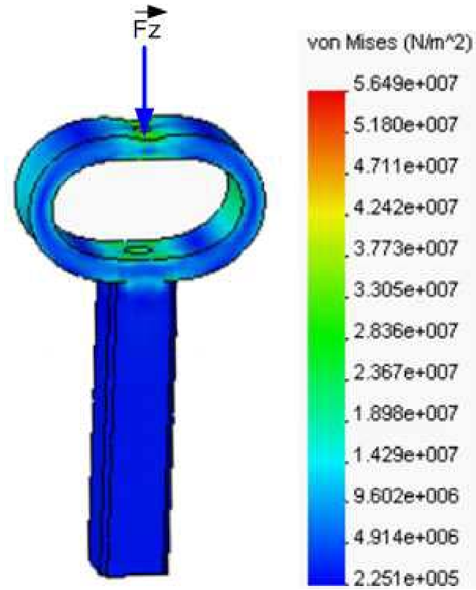

Figure 6. Stress result of *Fz* comprising force

IV. A 3D FORCE SENSOR REALIZATION

The realization of the 3D force sensor is depicted schematically in figure.7. The sensor is composed of eight strain gauges configured in three Wheatstone bridges. The transducer has a proving ring for measuring vertical force *Fz* and squared portion for measuring the horizontal forces *Fx* and *Fy*. These parts were machined separately and assembled together for reducing the complexity of machining the whole sensor. The effort exerted on the sensor is converted into an output signals. This conversion is realized with eight strain gauges mounted on metallic test body. The process of gluing the gauge is common and in our case commercial glue (cyanocrylate)™ was used for this purpose owing to the lack of special glue. The surface of the test body was well polished with an appropriate abrasive paper (No 500/1000) and cleaned with an acetone solution in order to remove all dirties. Once the test body is prepared, a small drop of glue is applied to the cleaned surface and just after a few seconds the gauges are clasped at the test body. To avoid the stick out of the gauge's wires, a small flexible PCB (Printed Circuit Board) is used for soldering the external wires not directly to the gauges. The gauges chosen are 7x5 mm from Micromeasurement® with a gauge factor and resistance 2 and 120 Ω respectively. The gauge's resistance value is known with a precision less than 0.01% because of the very low stress, which induces very low resistance variation.

Figure 7. The 3D force sensor realization

a. The conditioning circuit

The conditioning circuit for the 3D force sensor is depicted schematically in figure.8. The strain gauges in each Wheatstone bridge convert the resistance change to differential voltage. The stress applied on the transducer is expressed in μStrain (μm/m). The gauges are wired together to form a Wheatstone bridge with equal resistance. The expression of the final voltage at the output bridge will be directly linear with the applied stress [13]. The output signal issued from the bridge is carried onto an instrumentation amplifier realized using the operational amplifiers (AD622) with a low offset voltage and a high common mode rejection ratio (CMRR). The bridge is obviously supplied by a special voltage reference with higher precision (less than 0.002%) to avoid noise, which could arise at the same magnitude of the desired signal. Also, the resistances for gain adjustment are chosen for their high precision and low drift against temperature. After amplifications, each signal is feed at a pass filter constituted by a second order Butterworth filter with 1 kHz cut-off frequency. The signals issued from the three Wheatstone bridges are carried in to the commercial National Instrument (DaqBoard 1005) data acquisition card with PCI interfacing to a compatible PC. In addition, the use of shielding and guarding cable permitted a strong decreasing of extrinsic noise. figure.9 shows the realization of conditioning circuit.

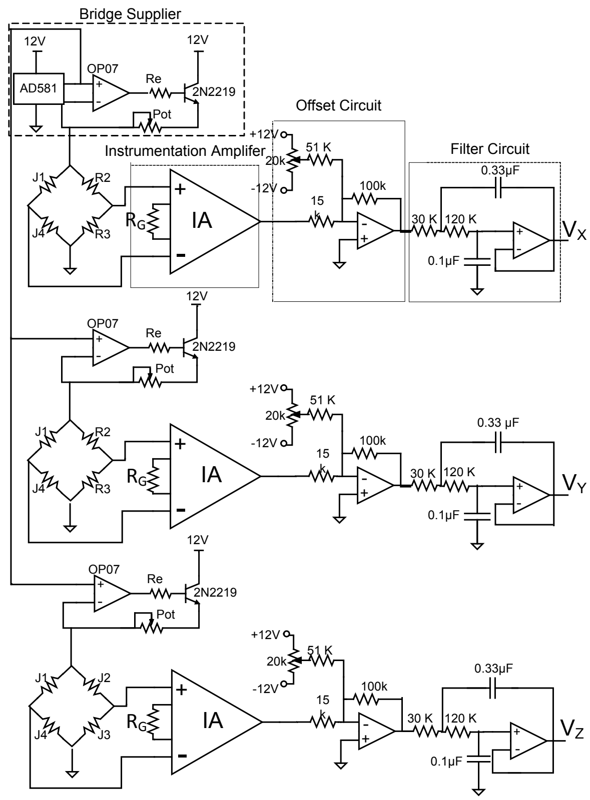

Figure 8. The conditioning Circuit

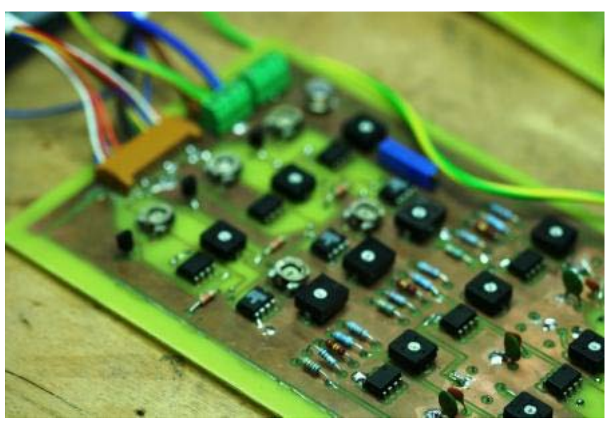

Figure 9. The realization card of conditioning Circuit

b. Sensor Calibration

The sensor calibration was performed by exerting different weights on the transducer in each axis (figure.10), and the three output voltages were recorded. For *Fz* force calibration, the z-axis was kept vertical and the other two axes were horizontal. The *Fx* force calibration was with the z-axis and y-axis kept horizontal, and the *Fy* force calibration was with the z-axis and x-axis kept horizontal. The gain and linearity for each axis were calculated by linear regression (figure.11), (figure.12) and (figure.13).

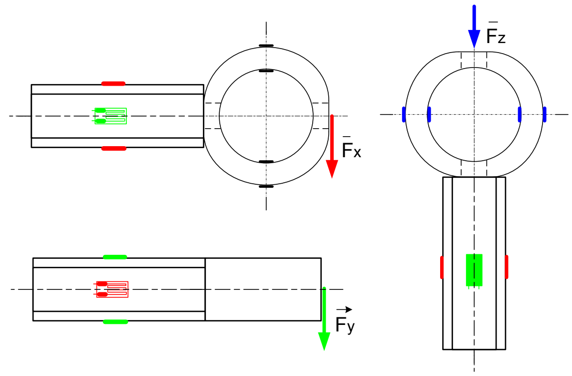

Figure 10. A 3D Sensor position for calibration

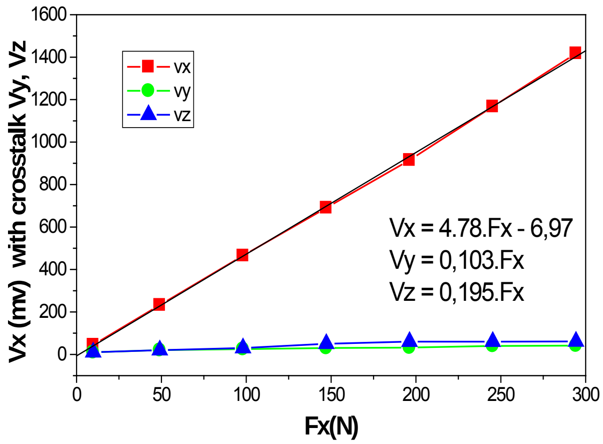

Figure 11. Results of the *Fx* force calibration

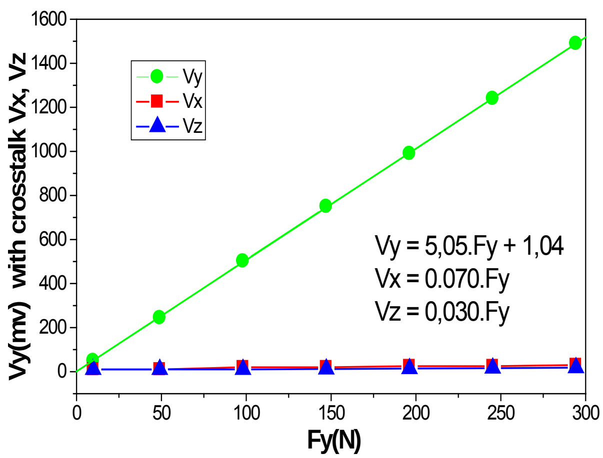

Figure12. Results of the *Fy* force calibration

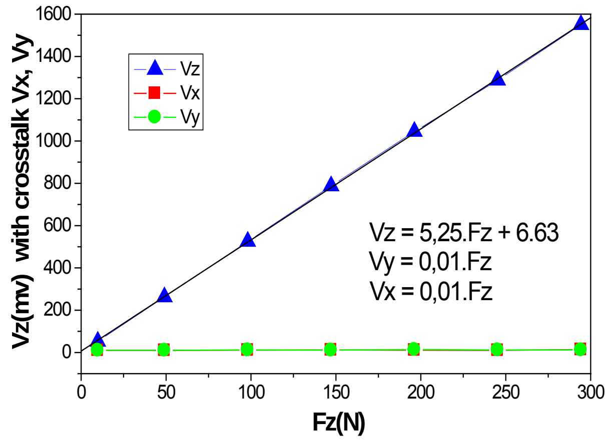

Figure 13. Results of the *Fz* force calibration

The data result of the calibrations shows a good correlation coefficient of linear fitness, 0.9999 for F_Z, and 0.9997 for F_X and F_Y. However, the sensor prototype is an easy innovative made instrument for measuring the 3D force. Futures investigations are oriented toward the realization of 3D force platform system for the ground reaction forces measurements in human dynamic analysis.

V. CONCLUSION

A new 3D force sensor developed using strain gauge is proposed for measuring three-directional reaction forces. Finite element method was adopted to optimize the structure dimensions, and improve the sensitivity of force sensor by distributing the sensing stress on the maximum strain positions. A hardware circuit including amplifiers module and conditioning circuits was developed for the force sensor. The calibration experiments were performed to calculate calibration coefficients by using the regression analysis method and test linear property of the sensor. The calibration data shows a good correlation coefficient of linear fitness, 0.9999 for F_Z, and 0.9997 for F_X and F_Y. In the future works, the 3D force sensor will be attached on bioinstrumentation system for ground reaction forces measurements in human dynamic analysis.

REFERENCES

[1] C.M. kim and J.J. Eng, “Magnitude and pattern of 3D kinematic and kinetic gait profiles in persons with stroke: relationship to walking speed,” Gait and Posture, vol. 20, pp. 140-146, 2004.

[2] M. Casadio, P.G. Morasso and V. Sanguineti, “Direct measurement of ankle stiffness during quiet standing: implications for control modelling and clinical application,” Gait and Posture, vol. 21, pp. 410-424, 2005.

[3] Eiji Matsumoto and Yuji Komagome, “Intelligent structural elements covered by piezoelectric high-polymer film,” International Journal on Smart Sensing and Intelligent Systems, s2is, www.s2is.org, vol. 1, no. 2, June 2008.

[4] S. Boukhenous and M. Attari, “A plantar pressure instrument for ankle rehabilitation,” in Proc. 4th International Conference on Sensing Technology, ICST’2010, Lecce, Italy, pp. 492-494, June 3-5, 2010.

[5] S. Boukhenous and M. Attari, “A low cost instrumentation based sensor array for ankle rehabilitation,” Chapter Book: Biomedical Engineering, trends in Electronics, Communications and Software,ISBN 978-953-307-475-7,InTech Publicher,www.InTech.Org, pp. 69-78, Jan 2011.

[6] L. Beccai, S. Roccella, A. Arena, F. Valvo, P. Valdastri, A. Menciassi, M.C. Carroza and P. Dario “Design and fabrication of hybrid silicon three-axial force sensor for biomechanical applications,” Sensors and Actuators A: Physical, vol. 120, pp. 370-382, 2005.

[7] R.K. Begg, S.M. Rahman, “A Method for the reconstruction of ground reaction force-time characteristics during gait from force platform recordings of simultaneous foot falls,” IEEE Trans. Biomed. Eng., vol. 47, no.4, pp 547-551, 2000.

[8] S. Boukhenous, M. Attari and N. Ababou, “A dynamic study of a foot-to-floor interaction during a vertical jumping,” AMSE journals, vol. 75, no. 1, pp. 41- 49, 2006.

[9] S. Boukhenous, M. Attari and N. Ababou, “A strain gauges platform for vertical jumping study,” Seventh International Symposium on Signal Processing and its Applications, IEEE-ISSP’2003, Paris, France, ISBN 0-7803-7946-2, vol.2, pp. 13-16, July 2003.

[10] E. Vazsonyi, M. Adam, Cs. Dusco, Z. Vizvary, A. L. Toth and I. Barsony, “Three-dimensional force sensor by novel alkaline etching technique,” Sensors and Actuators: A. Physical, vol. 123-124, pp. 620-626, 2005.

[11] Z. Jin and R. Kobetic, “Rail Supporting Transducer Posts for Three-Dimensional Force Measurement,”IEEE Trans. On Rehab. Eng, vol. 5, no. 4, pp. 380-387, Dec. 1997.

[12] W.C. Young, Roark’s Formulas for Stress and Strain, 6th Edition, New York, McGraw-Hill, 1989.

[13] J. G. Webster, Handbook of Measurement Instrumentation Sensors, CRC Press LLC, 1999.